THE JOURNAL OF BIOLOGICAL CHEMISTRY VOL. 285, NO. 53, pp. 41517–41524, December 31, 2010

Identification of Low Molecular Weight Pyroglutamate Aβ Oligomers in Alzheimer Disease

A NOVEL TOOL FOR THERAPY AND DIAGNOSIS[*S]

Received for publication, August 25, 2010, and in revised form, October 18, 2010 Published, JBC Papers in Press, October 22, 2010, DOI 10.1074/jbc.M110.178707

Oliver Wirths[‡], Christian Erck[§], Henrik Martens[§], Anja Harmeier[¶], Constanze Geumann[§], Sadim Jawhar[‡], Sathish Kumar[‖], Gerd Multhaup[¶], Jochen Walter[‖], Martin Ingelsson[**], Malin Degerman-Gunnarsson[**], Hannu Kalimo[‡‡], Inge Huitinga[§§1], Lars Lannfelt[**], and Thomas A. Bayer[‡2]

From the [‡]Department of Molecular Psychiatry and Alzheimer, Graduate School, University Medicine Goettingen, 37075 Goettingen, Germany, [§]Synaptic Systems, 37079 Göttingen, Germany, the [¶]Institute of Chemistry and Biochemistry, Free University of Berlin, 14195 Berlin, Germany, the [‖]Department of Neurology, Molecular Cell Biology, University of Bonn, 53127 Bonn, Germany, the [**]Department of Public Health and Caring Sciences Rudbeck Laboratory, Uppsala University, SE 75185 Uppsala, Sweden, the [‡‡]Department of Pathology, University of Helsinki, FI-00014 Helsingin yliopisto, Finland, and the [§§]Netherlands Brain Bank, Netherlands Institute for Neuroscience, 1105 BA Amsterdam, Netherlands

N-terminally truncated Aβ peptides starting with pyroglutamate (AβpE3) represent a major fraction of all Aβ peptides in the brain of Alzheimer disease (AD) patients. AβpE3 has a higher aggregation propensity and stability and shows increased toxicity compared with full-length Aβ. In the present work, we generated a novel monoclonal antibody (9D5) that selectively recognizes oligomeric assemblies of AβpE3 and studied the potential involvement of oligomeric AβpE3 *in vivo* using transgenic mouse models as well as human brains from sporadic and familial AD cases. 9D5 showed an unusual staining pattern with almost nondetectable plaques in sporadic AD patients and non-demented controls. Interestingly, in sporadic and familial AD cases prominent intraneuronal and blood vessel staining was observed. Using a novel sandwich ELISA significantly decreased levels of oligomers in plasma samples from patients with AD compared with healthy controls were identified. Moreover, passive immunization of 5XFAD mice with 9D5 significantly reduced overall Aβ plaque load and AβpE3 levels, and normalized behavioral deficits. These data indicate that 9D5 is a therapeutically and diagnostically effective monoclonal antibody targeting low molecular weight AβpE3 oligomers.

Alzheimer disease (AD)[3] represents the most frequent form of dementia and is characterized by the presence of extracellular amyloid plaques composed of amyloid-β (Aβ) surrounded by dystrophic neurites and neurofibrillary tangles. The discovery that certain early-onset familial forms of AD may be caused by enhanced levels of Aβ peptides have led to the hypothesis that amyloidogenic Aβ is intimately involved in the AD pathogenic process (1). In the past extracellular Aβ has been regarded as the major culprit, whereas more recent evidence now points to toxic effects of Aβ in intracellular compartments (2–3). In addition, other concepts propose that the soluble oligomers and the β-sheet containing amyloid fibrils are the toxic forms of Aβ (4–6). Supporting this notion, it has been demonstrated that soluble oligomeric Aβ42, but not plaque-associated Aβ, correlates best with cognitive dysfunction in AD (7–8). Oligomers are formed preferentially intracellulary within neuronal processes and synapses rather than extracellularly (9–10). Besides full-length Aβ peptides starting with an aspartate at position 1, a variety of different N-truncated Aβ peptides have been identified in AD brains. Ragged peptides including phenylalanine at position 4 of Aβ have been reported as early as 1985 by Masters *et al.* (11). In contrast, no N-terminal sequence could be obtained from cores purified in a sodium dodecyl sulfate-containing buffer, which led to the assumption that the N terminus could be blocked (12–13). The presence of AβpE3 (N-terminally truncated Aβ starting with pyroglutamate) in AD brain was subsequently shown using mass spectrometry of purified Aβ peptides, explaining at least partially initial difficulties in sequencing Aβ peptides purified from human brain tissue (14). The authors reported that only 10–15% of the total Aβ isolated by this method begins at position 3 with AβpE3. Saido *et al.* (15) subsequently showed that AβpE3 represents a dominant fraction of Aβ peptides in senile plaques of AD brains. Recently, we generated a new mouse model selectively expressing AβpE3–42 in neurons, and demonstrated for the first time that this peptide is neurotoxic *in vivo* leading to neuron loss and an associated neurological phenotype (16). Recently, it has been demonstrated that the N-terminal pE-formation can be catalyzed by glutaminyl cyclase (QC), which can be pharmacologically inhibited by QC inhibitors, both *in vitro* (17) and *in vivo* (18). QC expression was found up-regulated in the cortex of patients with AD and correlated with the appearance of pE-modified Aβ. Oral application of a QC inhibitor resulted in reduced AβpE3–42 burden in two different transgenic mouse models of AD as well as in a transgenic

* This work was supported by the German Federal Ministry for Economy (to T. A. B., C. E., and H. M.) and the Fritz Thyssen Stiftung (to O. W.).
[S] The on-line version of this article (available at http://www.jbc.org) contains supplemental Figs. S1–S7 and Table S1.
[1] Represents the corporate authorship of the Netherlands Brain Bank.
[2] To whom correspondence should be addressed: Division of Molecular Psychiatry, University Medicine Göttingen, Von-Siebold-Strasse 5, 37075 Göttingen, Germany. E-mail: tbayer@gwdg.de.
[3] The abbreviations used are: AD, Alzheimer disease; APP, amyloid precursor protein; AβpE3, pyroglutamate Aβ; Aβ, amyloid-β; QC, glutaminyl cyclase; SEC, size exclusion chromatography.

Drosophila model. Interestingly, treatment of these mice was accompanied by reductions in Aβx-40/42, diminished plaque formation and gliosis, as well as improved performance in context memory and spatial learning tests (18). Thus, AβpE3–42 variants are promising targets in both therapeutic and diagnostic strategies of AD.

EXPERIMENTAL PROCEDURES

Antibodies—The AβpE3 oligomer specific antibodies 9D5 (IgG2b; official name of cell line PG3–38 9D5H6) and 8C4 (IgG1; official name of cell line PG3–38 8C4D2) were generated by the University Medicine Goettingen and Synaptic Systems (Goettingen, Germany) by immunizing three Balb/c mice with AβpE3–38 (supplemental Fig. S1). After preparation of the lymph nodes cells were fused with the myeloma cell line P3-X63-Ag8. The hybridoma supernatants of mixed clones were screened by ELISA and subcloned. The monoclonal antibodies 9D5 and 8C4 were selected by ELISA against different N-terminal Aβ epitopes. Clones producing signals with AβpE3–38 and AβpE3–42, but no signal with AβpE1–42 were isolated and further characterized. For comparison, Aβ antibodies 4G8 (Aβ epitope 17–24; Covance), W0–2 (Aβ epitope 5–8; The Genetics Company), G2–10 (Aβ epitope x-40; The Genetics Company), G2–11 (Aβ epitope x-42), NT78 (against generic Aβ1–16, Synaptic Systems), and 2–48 (against N-terminal AβpE3, Synaptic Systems (19)) were used. The specific binding to AβpE3–42 and not to AβpE3–7has been demonstrated in an ELISA assay (supplemental Fig. S2). GFAP (rabbit) and IBA1 (rabbit) antisera were from Synaptic Systems and Wako Pure Chemicals, respectively.

Size-exclusion Chromatography (SEC) followed by Dot Blot—Prior to experiments, synthetic Aβ peptides (Peptide Speciality Laboratory) were monomerized in 98% formic acid (20). After immediate evaporation of the solvent, peptides were dissolved to 1 mg/ml in 0.1% ammonia following ultrasonic treatment. Size-exclusion chromatography was performed using a Superdex 75 (10/30HR) column (Amersham Biosciences). Aliquots of freshly dissolved 0.2 mg of synthetic peptide were loaded, and 0.5-ml fractions were eluted with 1× PBS (137 mM NaCl, 2.7 mM KCl, 10 mM Na_2HPO_4, 2 mM KH_2PO_4) at a flow rate of 0.5 ml/min. For detection of Aβ peptides by dot blot, fractions were spotted on 0.2-μm nitrocellulose and either detected by monoclonal W0–2 or 9D5 antibody. Different batches of Aβ peptides were used to exclude individual differences, which were not observed throughout all studies. The SEC peaks were calibrated using the following molecular weight standards of the column: blue dextran (>200 kDa); bovine serum albumin (67 kDa); ovalbumin; (43 kDa); chymotrypsinogen (25 kDa); RNaseA (13.7 kDa); aprotinin (6.5 kDa), and vitamin B12 (1.35 kDa). The corresponding stoichiometries were calculated and expressed as previously published (6, 21–22).

Western Blotting of Synthetic Peptides—For Western blot analysis, 1.5 μg of peptides were loaded on 4–12% vario gels (Anamed), transferred to 0.45 μm nitrocellulose membranes and detected using the primary antibodies W0–2 (1 μg/ml) and 9D5 (10 μg/ml) in blocking buffer. The blots were developed using enhanced chemiluminescence.

Thioflavin T Aggregation Assay—Peptides were solubilized in 10 mM NaOH at a concentration of 1 mg/ml, sonicated for 5 min, frozen in liquid nitrogen, and stored at −80 °C until use. Aggregation of Aβ peptides was investigated online using ThT aggregation assay (Varian fluorescence spectrophotometer) using an excitation wavelength of 446 nm and emission wavelength of 482 nm. Samples contained 55 μM Aβ, 50 mM sodium phosphate buffer (pH 7.4), 50 mM NaCl, 20 μM ThT, and 0.01% sodium azide. The samples were incubated at 37 °C in a peltier adapter with stirring. Data points were recorded every 10 min during the assay.

Toxicity of Peptides on Neuroblastoma Cells—Toxicity was verified as previously published (6). Briefly, SH-SY5Y neuroblastoma cells were routinely cultured. After 48 h, medium was replaced by medium containing freshly dissolved peptides, each at 2 μM concentration in the presence or absence of 1 ng/μl 9D5 antibody and incubated for 12 h. Cell viability was determined using MTS assay (Promega), according to the manufacturer's instructions compared with vehicle-treated control cells.

ELISA of AβpE Oligomers in Plasma—Plasma samples (stored at −70 °C) from patients with AD and healthy controls (HC) were analyzed. The patients were recruited at the Memory Clinic at the Department of Geriatrics, Uppsala University Hospital. All AD patients were diagnosed according to DSM IV and NINCDS-ADRDA. AβpE oligomer levels in human plasma samples were measured by ELISA according to standard methods. Briefly 9D5 antibody was coated as capture antibody and blocked with 5% skimmed milk, 0.05% Tween in PBS. Biotinylated antibody 2–48 against pE-Aβ in combination with streptavidin-HRP and the chromogen TMB (Pierce) was used for detection.

ELISA of AβpE Levels in Brain—Frozen brains were homogenized in a Dounce homogenizer in TBS (120 mM NaCl, 50 mM Tris pH 8.0 containing complete protease inhibitor (Roche)), and subsequently centrifuged at 27.000 g for 20 min at 4 °C. The resulting pellets were resuspended in 2% SDS, sonified and centrifuged for 15 min. AβpE levels were measured by ELISA according to standard methods. NT78 (against Aβ1–16) antibody was coated as capture antibody. Biotinylated antibody 2–48 (against N-terminal AβpE3) was used as detection antibody in combination with streptavidin-HRP and the chromogen TMB (Pierce).

Human Brain Samples—Human brain samples were obtained from the Netherlands Brain Bank (NBB), Hopital del la Salpetrière (a generous gift of Prof. Dr. Charles Duyckaerts and Dr. Veronique Sazdovitch), University Hospital Helsinki and from Uppsala University. Definite diagnosis was based on established criteria and informed consent was obtained from all subjects.

Transgenic Mice—APP/PS1KI (23) and 5XFAD (24) female bigenic mice have been described previously. All mice were backcrossed for more than 10 generations on a C57BL/6J genetic background and housed at a 12-h day/12-h night cycle with free access to food and water. For passive immunization 4.5-month-old 5XFAD mice were weekly injected with 250 μg

of 9D5 or PBS intraperitoneally for 6 weeks. 9D5 antibody was purified by protein G-agarose. 250-ml culture supernatant was applied to the column and allowed to drain through. The column was washed with 200 ml of PBS, and the antibodies were eluted with 0.1 M glycine (pH 2.5), neutralized with 100 μl of 1.5 M Tris/HCL buffer (pH 8.8). Samples were measured at 280 nm. Eluted IgG fractions containing the highest absorptions were pooled and dialyzed with PBS. PBS injection has been used previously as a control for treatment effects of passive immunization of different AD mouse models with a variety of Aβ antibodies (25–29). All animals were handled according to German guidelines for animal care and studies were approved by the local legal authorities (LAVES).

Immunohistochemistry—Human and mouse tissue were processed as described previously (19). In brief, 4-μm paraffin sections were pretreated with 0.3% H_2O_2 in PBS to block endogenous peroxidases, and antigen retrieval was achieved by boiling sections in 0.01 M citrate buffer pH 6.0, followed by 3-min incubation in 88% formic acid. Primary antibodies were incubated overnight, followed by incubation with biotinylated secondary antibodies (DAKO) before staining was visualized using the ABC method with the Vectastain kit (Vector Laboratories) and diaminobenzidine (DAB) as chromogen. Alternatively, fluorochromated secondary antibodies (anti-mouse AlexaFluor594 and anti-rabbit AlexaFluor488, Invitrogen) were used for immunofluorescence detection.

Quantification of Plaque Load—Extracellular Aβ load (4G8, G2–10, G2–11, 2–48) was evaluated in cortex and hippocampus using an Olympus BX-51 microscope equipped with an Olympus DP-50 camera and the ImageJ software (V1.41, NIH). Serial images of 40× magnification (hippocampus) and 100× (cortex) were captured on six sections per animal, which were 30 μm afar from each other. Using ImageJ the pictures were binarized to 16-bit black and white images and a fixed intensity threshold was applied defining the DAB staining.

Behavioral Testing—Anxiety levels were assessed using an elevated plus maze as described previously (30). The percentage of the time spent in the open arms to the overall time and the ratio of the open arms to the total arms entries were measured using an automatic video tracking system (VideoMot2, TSE-Systems).

Statistical Analysis—Statistical differences were evaluated using one-way ANOVA followed by Bonferroni post-hoc test or unpaired *t* test as indicated. All data are given as means ± S.E. of the mean (S.E.). All statistics were calculated using GraphPad Prism V5.00 software.

RESULTS

Generation and Characterization of Antibodies Selectively Detecting AβpE3 Oligomers—Two mouse monoclonal antibodies (9D5 and 8C4) were identified with similar binding characteristics. Because 9D5 and 8C4 were competing for the same epitope in dot blot analysis and showing an indistinguishable staining pattern using immunohistochemistry (supplemental Fig. S1), only 9D5 was studied in greater detail. To analyze the binding properties of the oligomeric AβpE3 antibody (9D5), we performed SEC under native conditions with N-terminally truncated and modified AβpE3–42 and wild-type Aβ1–42 peptides followed by dot blot analysis. SEC of Aβ1–42 showed dominant peaks of low-n oligomers (4–6×) with some higher (16–20×) and few smaller (1–2×) aggregates (6, 21, 31–35). In contrast, SEC of AβpE3–42 yielded high levels of smaller forms (1–2×), low-n oligomers (4–6×) and lower levels of higher oligomeric aggregates (10–20×), indicating differential aggregation characteristics of Aβ1–42 and AβpE3–42. All Aβ1–42 and AβpE3–42 SEC fractions were recognized by the generic Aβ antibody W0–2 in a dot blot analysis, however, the 9D5 antibody detected only low-n oligomeric fractions (4–10×) of AβpE3–42, whereas no signal was obtained using the Aβ1–42 fractions (Fig. 1, *A* and *B*). Under denaturing conditions 9D5 detected one single band of low molecular weight (LMW) AβpE3–42 without any cross reactivity for Aβ1–42. As expected, W0–2 detected a range of aggregation states of Aβ1–42 peptides as well as monomeric Aβ1–42 (Fig. 1*C*). Together, these data demonstrate that 9D5 is highly selective for lower oligomeric variants of AβpE3–42.

Antibody 9D5 Inhibited Aggregation and Toxicity in Vitro—The aggregation of monomeric Aβ1–42 and AβpE3–42 peptides (55 μM) was investigated using a ThT fluorescence assay. While Aβ1–42 showed the expected aggregation profile with a pronounced lag phase before fibril growth, AβpE3–42 showed very rapid formation of intermediate oligomeric assemblies. Interestingly, elongation rates of AβpE3–42 were much slower as that of Aβ1–42 (*Fig. 1D*). These data indicate that AβpE3–42 rapidly formed intermediate oligomeric assemblies, but has decreased propensity to form larger fibrils, a behavior that clearly differs from that of that of Aβ1–42. Notably, the presence of antibody 9D5 efficiently decreased the formation of higher aggregates of the AβpE3–42 peptide at a 1:76 (9D5:Aβ) ratio, but not the rapid formation of lower oligomers, further demonstrating the specificity of this antibody for lower oligomeric species of AβpE3 and its efficiency in the inhibition of further peptide aggregation (Fig. 1*E*). This observation suggests that 9D5 inhibits the formation of higher Aβ aggregates by binding to LMW oligomers as indicated in SEC and Western blot experiments. We next studied the toxicity of Aβ1–42 and AβpE3–42 peptides in SH-SY5Y neuroblastoma cells. To determine whether the toxic effect of AβpE3–42 can be influenced by 9D5 antibody, we incubated neuroblastoma cells either with Aβ1–42, AβpE3–42 or with peptides and 9D5. Application of both, AβpE3–42 and 9D5 completely abolished the toxic effect of AβpE3–42. This effect is highly specific, as application of Aβ1–42 together with 9D5 caused the same effect on cell viability as Aβ1–42 incubation alone (Fig. 1*F*).

Antibody 9D5 Shows a Specific Staining Profile in Alzheimer Brain—9D5 was used to characterize the distribution of oligomeric AβpE in human post-mortem brain tissue (frontal cortex and hippocampus from sporadic AD, familial AD (FAD) and non-demented individuals) (Fig. 2, supplemental Table S1 and Fig. S7). While none of the non-demented controls showed plaque staining with 9D5, some specimen showed plaque staining using 4G8 (against Aβ17–24). Occasionally

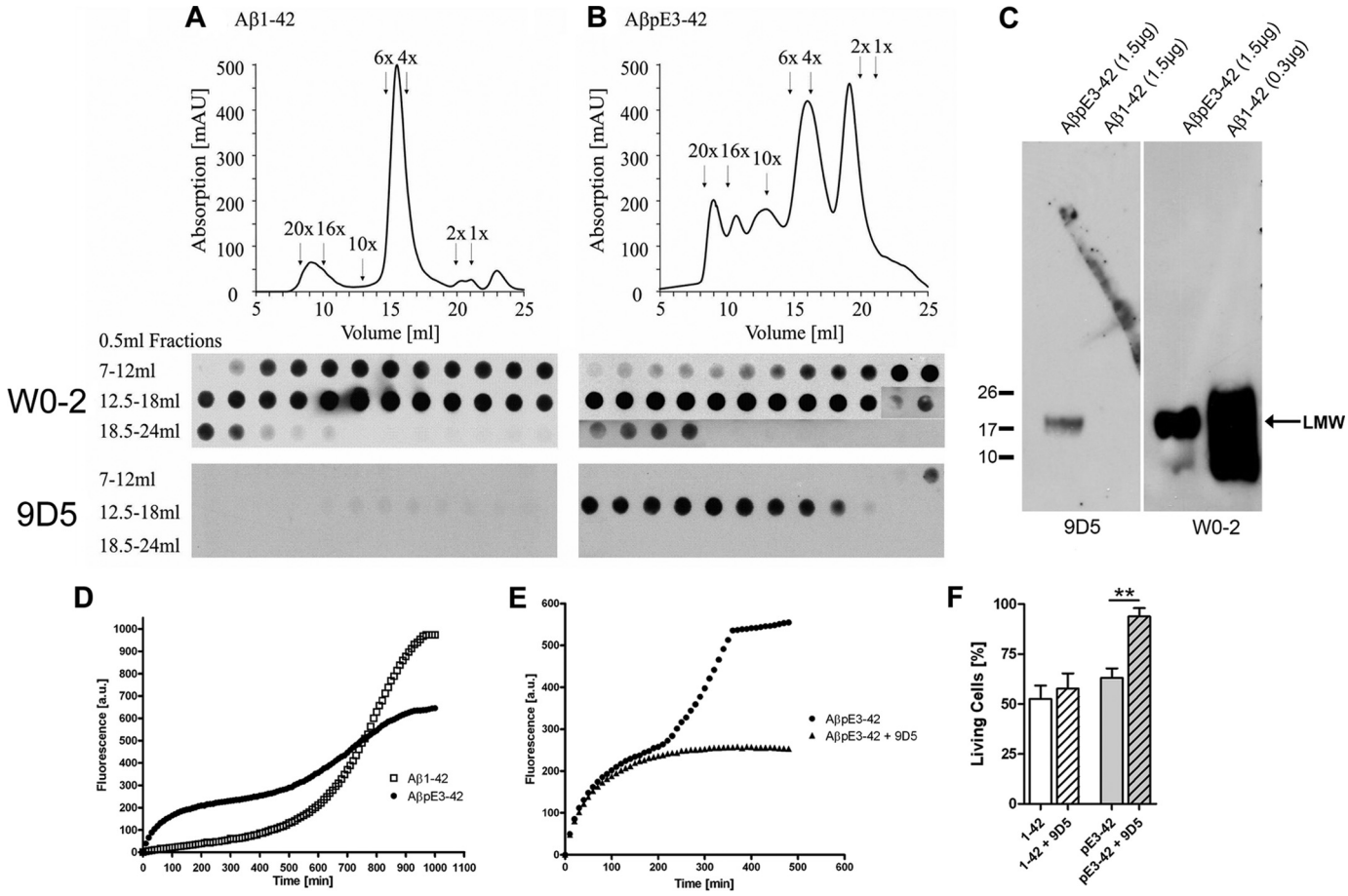

FIGURE 1. **9D5 recognized AβpE3 oligomers and inhibited AβpE3 aggregation *in vitro*.** *A*, Aβ1–42 peptides formed mainly low-n oligomers (4–6×) and only minor amounts of higher aggregates (10–20×) and monomers and dimers (1–2×). All Aβ1–42 forms were detectable by dot blot with W0–2, whereas 9D5 did not show any signal. *B*, separation profile of AβpE3–42 peptides showed high amounts of monomers to hexamers (1–6×) and lower amounts of higher aggregates (10–20×). Again, W0–2 recognized all aggregation forms of AβpE3–42 with different sensitivity (Note, longer exposure of AβpE3–42 fractions 17–24 ml). 9D5 however solely detected low-n oligomers (4–10×) and no smaller or larger oligomers. *C*, under reducing conditions 9D5 recognized a single band of low molecular weight (LMW) oligomeric AβpE3–42. No signal was detected in the Aβ1–42 lane. W0–2 recognized LMW AβpE3–42 and Aβ1–42 oligomers. *D*, aggregation kinetics of Aβ1–42 and AβpE3–42 monitored by ThT fluorescence. Aggregates were very rapidly generated from AβpE3–42, indicating an instant seeding of the aggregation process. Aβ1–42 showed a typical lag phase, *i.e.* the phase in which oligomers and protofibrils are slowly formed, whereas AβpE3–42 rapidly formed intermediate oligomeric assemblies, but has decreased propensity to form larger fibrils, a behavior that clearly differs from that of that of Aβ1–42. *E*, accelerated increase after the inflection point at 200 min was efficiently blocked by addition of 9D5 together with AβpE3–42. *F*, toxicity measurements of SH-SY5Y neuroblastoma cells incubated with Aβ1–42 and AβpE3–42 in addition with 9D5 antibody compared with vehicle control. Whereas Aβ1–42 (with and without 9D5) and AβpE3–42 displayed high toxic effects, AβpE3–42 in the presence of 9D5 is not toxic ($n = 3$–5; ANOVA, $p = 0.0001$; followed by *t* test, $p = 0.0048$).

weak 9D5 blood vessel immunostaining was observed. This observation demonstrated that plaques in healthy controls do not harbor the 9D5 epitope and indicates that plaques in nondemented controls do not contain oligomeric AβpE3. In contrast, most of the sporadic AD and FAD cases demonstrated high abundance of intraneuronal and cerebral amyloid angiopathy (CAA) staining with 9D5 (Fig. 2, *A* and *B*), clearly differing from the 4G8 pattern (*e.g.* sporadic case 1 and 2, Fig. 2*A*). FAD cases having mutations in the APP gene (Swedish or arctic mutation) revealed abundant 9D5 immunoreactivity. Of interest, all analyzed FAD cases harboring mutations in the presenilin-1 gene (P264L, L418F, PS1Δexon9) showed prominent intraneuronal 9D5 immunoreactivity (Fig. 2*B*, supplemental Table S1). Oligomeric AβpE3–42 antibody 9D5 showed a specific staining pattern different from the staining pattern with an antibody against the N terminus of AβpE3–42 (supplemental Fig. S3).

Lower Levels of Oligomeric AβpE3 in Plasma of Alzheimer Patients—To assess the diagnostic potential of oligomeric AβpE3 variants and antibody 9D5, we established a novel ELISA and tested plasma of AD patients and healthy controls (HC). Interestingly, levels of AβpE3 oligomers were significantly reduced in AD patients by 46% as compared with healthy controls ($p < 0.05$) (Fig. 2*C*). We have previously published that the level of IgM autoantibodies in plasma directed against AβpE3 was significantly decreased in AD patients as compared with healthy controls. In good agreement with these observations, the signal of AβpE3 oligomers detected by 9D5 was significantly lower in plasma of AD patients again pointing out that 9D5 can be used as a biomarker tool for AD diagnosis (36). We hypothesize that lower levels of AβpE3 oligomers in plasma are due to development of cerebral amyloid angiopathy and increased accumulation within neurons (supplemental Fig. S6).

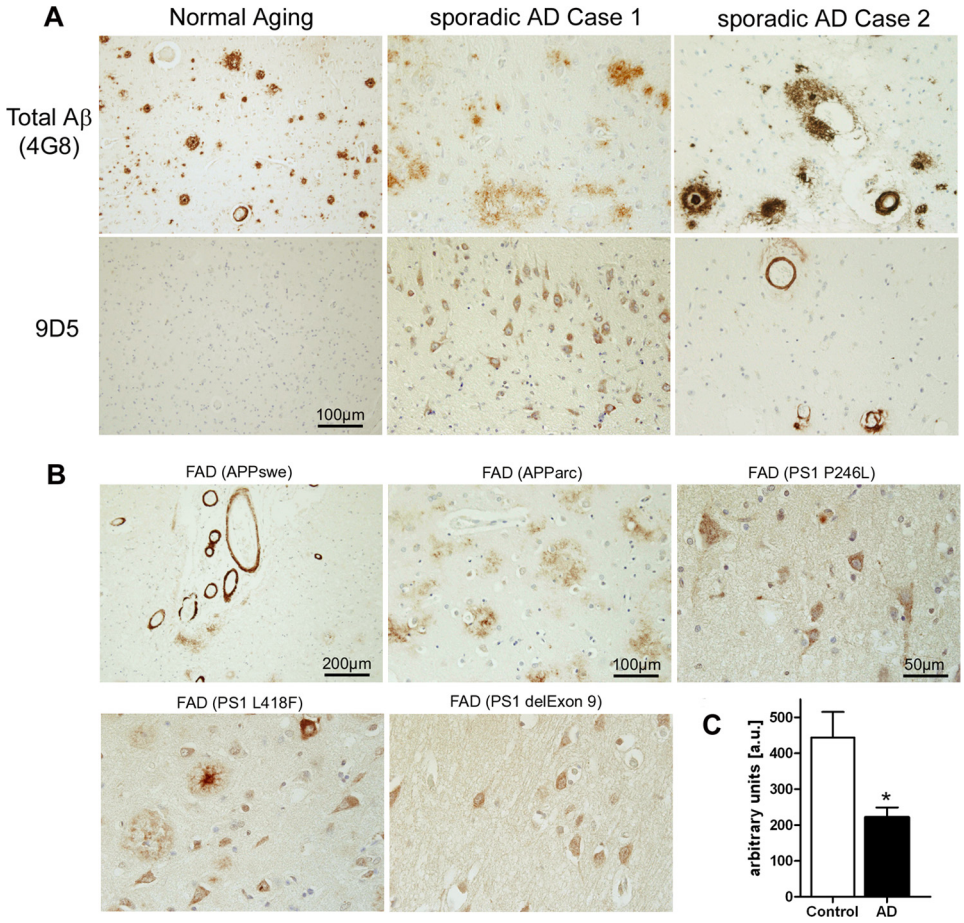

FIGURE 2. **9D5 diagnostically differentiates between sporadic AD cases and non-demented controls.** *A*, staining with antibody 9D5 detected either abundant intraneuronal imunoreactivity (sporadic case 1) and/or strong vascular staining (sporadic case 2) in sporadic AD cases, which clearly differentiate from 4G8 staining. Non-demented control cases were devoid of intraneuronal or extracellular 9D5 plaque immunoreactivity (normal aging case), despite of abundant 4G8-positive plaques. *B*, FAD cases with mutations in the APP gene (Swedish or arctic mutation) reveal abundant 9D5 immunoreactivity. Of interest, all FAD cases harboring mutations in the presenilin-1 gene (P264L, L418F, PS1Δexon9) showed prominent intraneuronal 9D5 immunoreactivity. *C*, plasma levels of AβpE3 oligomers. Sandwich ELISA with 9D5 as capture antibody and 2–48 as detector antibody demonstrating reduced plasma levels (in 50 μl of plasma) of AβpE3 oligomers in AD patients as compared with non-demented controls (unpaired *t* test, $p < 0.05$). The demographic data of individuals for the plasma assay was as follows: age; AD patients ($n = 16$; 78 ± 1.8) and non-demented controls ($n = 10$; 69 ± 1.4); MMSE; AD (11.4 ± 3.2) and controls (29 ± 0.3); sex; AD (3 male/13 female) and controls (5 male/5 female).

Antibody 9D5 Shows a Specific Staining Profile in Transgenic Alzheimer Mouse Models—We next asked the question whether oligomeric AβpE peptides could also be detected in transgenic mouse models for AD. Staining of 3-month-old 5XFAD mice did not show any immunoreactivity (Fig. 3*A*), whereas considerable staining was detected in the subiculum of 6-month-old 5XFAD mice (Fig. 3*B*), showing a dramatic increase at the age of 12 months (Fig. 3*C*). 9D5 detected only intracellular and no plaque-associated staining corroborating the staining pattern in AD patients. In addition, other brain areas like cortex, pons or brainstem nuclei stained strongly positive at that time point (not shown). A very similar age-dependent accumulation of AβpE3 was also observed in APP/PS1KI mice, another model with robust neuron loss and associated behavioral deficits (23, 37) (supplemental Fig. S4). Double-staining using 9D5 (red) and the astrocytic marker GFAP (green) in the subiculum of 12-month-old 5XFAD mice revealed almost no co-localization in astrocytes (Fig. 3*D*). On the other hand, double-staining using 9D5 (red) and the microglia/macrophage marker Iba-1 (green) showed a strong co-localization, suggesting oligomeric AβpE3 variants are internalized by microglia (*arrowheads*) (Fig. 3*E*). In addition, strong intraneuronal 9D5-immunoreactivity could be demonstrated (Fig. 3*F*, *arrows*). The finding of intraneuronal 9D5 staining is corroborated by strong 9D5-immunoreactivity in spinal cord motor neurons of aged APP/PS1KI mice (supplemental Fig. S4).

Therapeutic Effect of Passive Immunization with 9D5 in 5XFAD Mice—Next we studied a potential therapeutic effect of 9D5 using a passive immunization approach. 4.5-month-old 5XFAD (female) mice were weekly injected with 250 μg of 9D5 intraperitoneally for 6 weeks. 9D5 treatment significantly reduced generic Aβ, Aβ42, Aβ40, and AβpE3 plaque load in hippocampus (HC) and cortex (Ctx) (Fig. 4, *A* and *B*). In good agreement, 9D5 treatment significantly stabilized the performance in the elevated plus maze (Fig. 4*C*). Confirming the plaque load data, a significant reduction of AβpE3 levels was observed in both the TBS and SDS fraction of brain lysates after 9D5 immunization of 5XFAD mice (Fig. 4*D*). Passive immunization of 5XFAD mice with 9D5 showed reduction of the intracellular AβpE3–42 oligomers (supplemental Fig. S5).

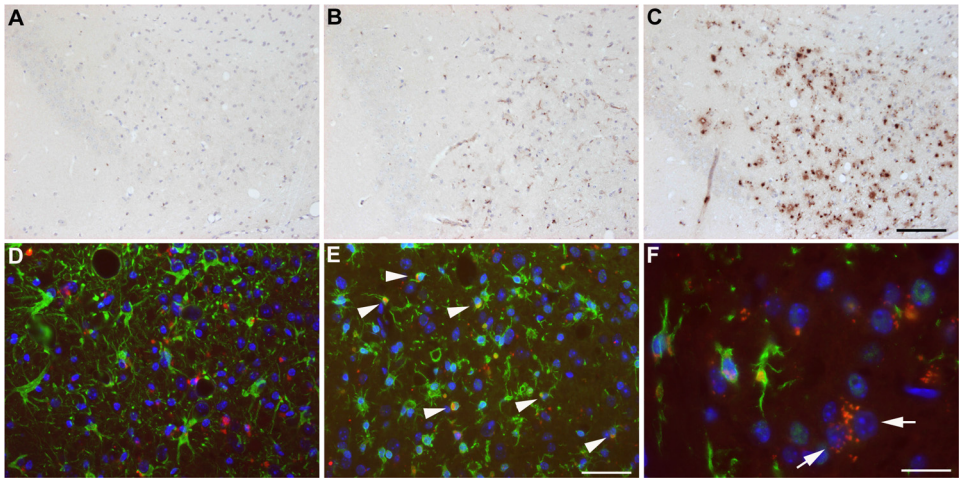

FIGURE 3. **Intracellular age-dependent staining of AβpE3 oligomers.** Staining with 9D5 in the subiculum of (*A*) 3-, (*B*) 6-, and (*C*) 12-month-old 5XFAD mice showing that the signal starts to appear at 6 months. *D*, double staining using 9D5 (*red*) and the astrocytic marker GFAP (*green*) in the subiculum of a 12-month-old 5XFAD mouse revealed no colocalization in astrocytes. *E*, in contrast, double-staining using 9D5 (*red*) and the microglia/macrophage marker Iba-1 (*green*) showed a strong colocalization in the subiculum of a 12-month-old 5XFAD mouse (*arrowheads*). *F*, strong intraneuronal 9D5-immunoreactivity could be demonstrated in the pons of a 12-month-old 5XFAD mouse.

DISCUSSION

Soluble oligomers (also described as ADDLs and/or protofibrils) of Aβ have been discussed to be causally involved in synaptic and cognitive dysfunction in the early stages of AD (38–39). However, there is no consensus on which aggregation state exerts the highest toxicity in AD. Nanomolar concentrations of small diffusible Aβ oligomers (17–27 kDa) cause neuronal death in hippocampal slice cultures (40) and Aβ dimers that were either cell-derived or extracted from AD brains impair synaptic plasticity (41). On the other hand, dodecameric Aβ56* oligomers extracted from the brain of APP transgenic mice interfere with learning and memory performance in rat (42). Analysis of neurotoxicity of oligomers ranging from monomers to tetramers of synthetic Aβ peptides demonstrated that tetramers have the strongest effect (43). The conclusion that oligomers are more potent candidates as pathogens is based primarily on experimental evidence demonstrating that natural and synthetic Aβ oligomers impair synaptic plasticity (40–41, 44), memory (33, 42, 44) and inducing loss of synapses (34, 45) when applied exogenously into rat cerebral ventricle, cultured brain slices, or dissociated neurons. It has been shown that soluble oligomeric Aβ42 and not plaque-associated Aβ correlate best with cognitive dysfunction (7–8). Aβ oligomers are formed preferentially intracellularly within neuronal processes and synapses rather than within the extracellular space (9–10). Tomiyama *et al.* generated APP transgenic mice expressing the E693Δ mutation, which causes neuronal cell death and cognitive impairment by enhanced Aβ oligomerization without fibrillization. The mice displayed age-dependent accumulation of intraneuronal Aβ oligomers from 8 months but no extracellular amyloid deposits even at 24 months. Hippocampal synaptic plasticity and memory were impaired at 8 months of age (46). Aβ protofibril levels correlate with spatial learning in AD transgenic mice expressing human APP with the arctic mutation (47) facilitating early intraneuronal Aβ aggregation (48). Despite the difficulty to compare the different studies on oligomeric Aβ species there seems to be converging evidence that they: 1) are primarily formed within neurons, 2) oligomeric Aβ species are more neurotoxic than monomeric or fibrillar Aβ *in vitro*, and 3) oligomeric Aβ species decrease synaptic activity.

In the present study, we have identified LMW AβpE3 oligomers, which can be detected by 9D5, a novel mouse monoclonal antibody. 9D5 did not cross react with any Aβ1–42 species indicating that these oligomers present a unique and novel epitope. The therapeutic potential of 9D5 was demonstrated in passively immunized 5XFAD mice as plaque load and Aβ levels were reduced and behavioral deficits were normalized. In an ELISA using 9D5 as capture antibody, we could show that the signal was significantly lower in plasma of AD patients as compared with non-demented controls. We believe that our observation represents a novel therapeutic mechanism rescuing AD pathology and related behavioral deficits. Several studies demonstrated that N-terminal specific Aβ antibodies showed significant beneficial effect in AD mouse models. Bard *et al.* (26) and Buttini *et al.* (49) studied the optimal antibody response for reducing neuropathology in PDAPP transgenic mice. Immune sera with reactivity against different Aβ epitopes and monoclonal antibodies with different isotypes were examined for efficacy and showed that antibodies against the N-terminal regions of Aβ were able to invoke beneficial effects. Saido *et al.* (15) suggested that AβpE3–42 is generated step-by-step from its precursor Aβ1–42 by N-truncation and glutamate to pyroglutamate formation. We therefore assume that reducing Aβ1–42 by passive immunization (reviewed in (50)) will also reduce AβpE3–42 levels and the resulting oligomeric forms. We think that AβpE3 oligomers represent an important pathological step appearing at a time point when behavioral deficits occur. Interrupting this toxic pathway by specifically reducing these oligomers also has an impact on other Aβ peptides as shown for example in reducing general plaque load. In conclusion, we have therefore demonstrated for the first time that oligomeric AβpE peptides represent a novel Aβ entity, which

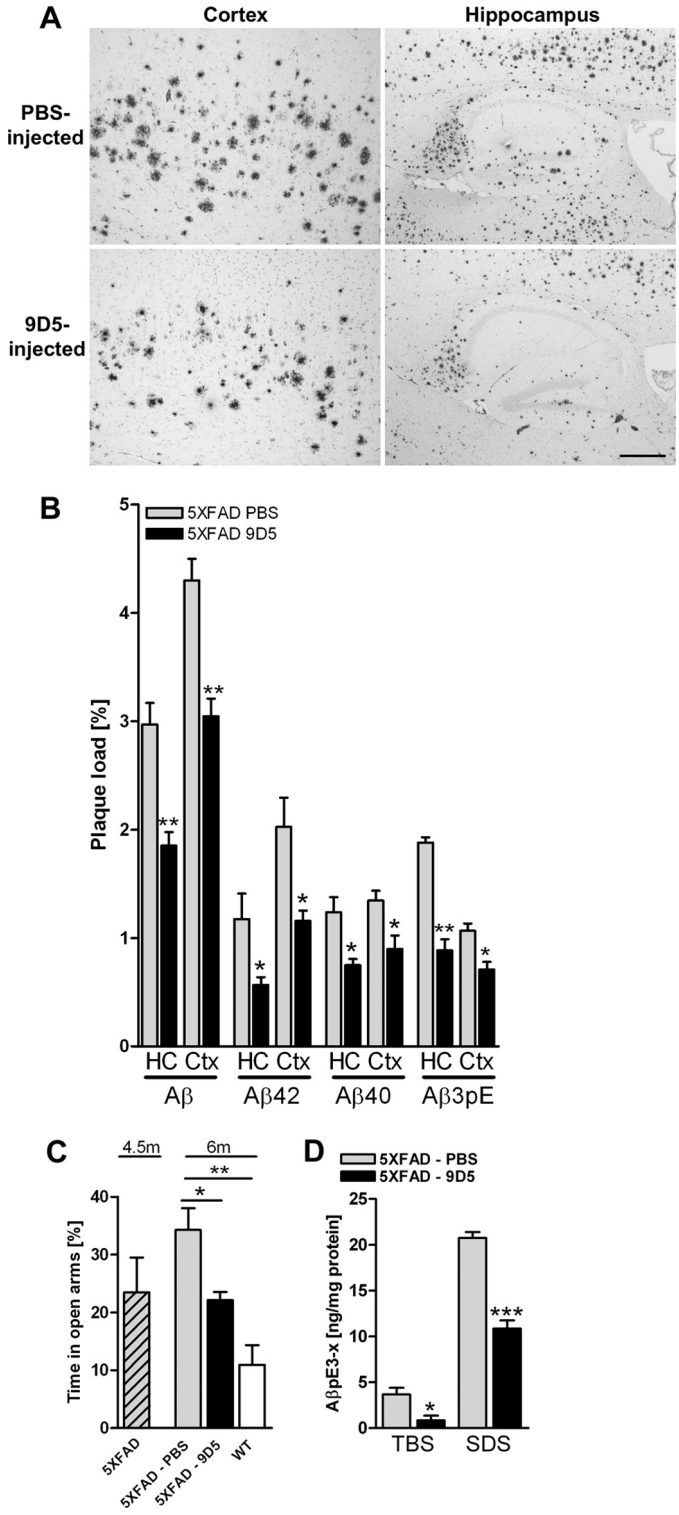

FIGURE 4. **Therapeutic effect of 9D5 passive immunization in 5XFAD mice.** *A*, plaque load in cortex and hippocampus using Aβ (4G8). *B*, plaque-load quantification showed a significant decrease for both total Aβ (4G8), Aβ40 (G2–10), Aβ42 (G2–11), and pyroglutamate-modified Aβ (2–48) in 9D5-injected mice compared with PBS-injected mice in both hippocampus (HC) and cortex (Ctx). *C*, importantly the elevated plus maze demonstrated stabilized anxiety levels after 9D5 treatment. *D*, ELISA analysis of Tris and SDS lysates of PBS and 9D5 injected 5XFAD mice demonstrated that 9D5 immunization reduced AβpE levels in both fractions significantly. In TBS lysates 9D5 immunization resulted in 77% reduced levels and SDS lysates resulted in 48% reduced levels (ANOVA of all groups; $p < 0.0001$). *, $p < 0.05$; **, $p < 0.01$; ***, $p < 0.001$ ($n = 4$ per group).

can be detected by specific antibodies serving as promising tools for diagnosis and therapeutic intervention of AD.

REFERENCES

1. Selkoe, D. J. (1998) *Trends Cell Biol.* **8,** 447–453
2. Tseng, B. P., Kitazawa, M., and LaFerla, F. M. (2004) *Curr. Alzheimer. Res.* **1,** 231–239
3. Wirths, O., Multhaup, G., and Bayer, T. A. (2004) *J. Neurochem.* **91,** 513–520
4. Selkoe, D. J. (2001) *Physiol. Rev.* **81,** 741–766
5. Klein, W. L. (2002) *Neurochem. Int.* **41,** 345–352
6. Harmeier, A., Wozny, C., Rost, B. R., Munter, L. M., Hua, H., Georgiev, O., Beyermann, M., Hildebrand, P. W., Weise, C., Schaffner, W., Schmitz, D., and Multhaup, G. (2009) *J. Neurosci.* **29,** 7582–7590
7. McLean, C. A., Cherny, R. A., Fraser, F. W., Fuller, S. J., Smith, M. J., Beyreuther, K., Bush, A. I., and Masters, C. L. (1999) *Ann. Neurol.* **46,** 860–866
8. Näslund, J., Haroutunian, V., Mohs, R., Davis, K. L., Davies, P., Greengard, P., and Buxbaum, J. D. (2000) *JAMA* **283,** 1571–1577
9. Walsh, D. M., Tseng, B. P., Rydel, R. E., Podlisny, M. B., and Selkoe, D. J. (2000) *Biochemistry* **39,** 10831–10839
10. Takahashi, R. H., Almeida, C. G., Kearney, P. F., Yu, F., Lin, M. T., Milner, T. A., and Gouras, G. K. (2004) *J. Neurosci.* **24,** 3592–3599
11. Masters, C. L., Simms, G., Weinman, N. A., Multhaup, G., McDonald, B. L., and Beyreuther, K. (1985) *Proc. Natl. Acad. Sci. U.S.A.* **82,** 4245–4249
12. Selkoe, D. J., Abraham, C. R., Podlisny, M. B., and Duffy, L. K. (1986) *J. Neurochem.* **46,** 1820–1834
13. Gorevic, P. D., Goñi, F., Pons-Estel, B., Alvarez, F., Peress, N. S., and Frangione, B. (1986) *J. Neuropathol. Exp. Neurol.* **45,** 647–664
14. Mori, H., Takio, K., Ogawara, M., and Selkoe, D. J. (1992) *J. Biol. Chem.* **267,** 17082–17086
15. Saido, T. C., Iwatsubo, T., Mann, D. M., Shimada, H., Ihara, Y., and Kawashima, S. (1995) *Neuron* **14,** 457–466
16. Wirths, O., Breyhan, H., Cynis, H., Schilling, S., Demuth, H. U., and Bayer, T. A. (2009) *Acta Neuropathol.* **118,** 487–496
17. Cynis, H., Scheel, E., Saido, T. C., Schilling, S., and Demuth, H. U. (2008) *Biochemistry* **47,** 7405–7413
18. Schilling, S., Zeitschel, U., Hoffmann, T., Heiser, U., Francke, M., Kehlen, A., Holzer, M., Hutter-Paier, B., Prokesch, M., Windisch, M., Jagla, W., Schlenzig, D., Lindner, C., Rudolph, T., Reuter, G., Cynis, H., Montag, D., Demuth, H. U., and Rossner, S. (2008) *Nat. Med.* **14,** 1106–1111
19. Wirths, O., Bethge, T., Marcello, A., Harmeier, A., Jawhar, S., Lucassen, P. J., Multhaup, G., Brody, D. L., Esparza, T., Ingelsson, M., Kalimo, H., Lannfelt, L., and Bayer, T. A. (2010) *J. Neural. Transm.* **117,** 85–96
20. Rohrer, D. C., Nilaver, G., Nipper, V., and Machida, C. A. (1996) *Cell Transplant.* **5,** 57–68
21. Klyubin, I., Walsh, D. M., Lemere, C. A., Cullen, W. K., Shankar, G. M., Betts, V., Spooner, E. T., Jiang, L., Anwyl, R., Selkoe, D. J., and Rowan, M. J. (2005) *Nat. Med.* **11,** 556–561
22. Fukumoto, H., Tokuda, T., Kasai, T., Ishigami, N., Hidaka, H., Kondo, M., Allsop, D., and Nakagawa, M. (2010) *Faseb J.* **24,** 2716–2726
23. Casas, C., Sergeant, N., Itier, J. M., Blanchard, V., Wirths, O., van der Kolk, N., Vingtdeux, V., van de Steeg, E., Ret, G., Canton, T., Drobecq, H., Clark, A., Bonici, B., Delacourte, A., Benavides, J., Schmitz, C., Tremp, G., Bayer, T. A., Benoit, P., and Pradier, L. (2004) *Am. J. Pathol.* **165,** 1289–1300
24. Oakley, H., Cole, S. L., Logan, S., Maus, E., Shao, P., Craft, J., Guillozet-Bongaarts, A., Ohno, M., Disterhoft, J., Van Eldik, L., Berry, R., and Vassar, R. (2006) *J. Neurosci.* **26,** 10129–10140
25. Bard, F., Cannon, C., Barbour, R., Burke, R. L., Games, D., Grajeda, H., Guido, T., Hu, K., Huang, J., Johnson-Wood, K., Khan, K., Kholodenko, D., Lee, M., Lieberburg, I., Motter, R., Nguyen, M., Soriano, F., Vasquez, N., Weiss, K., Welch, B., Seubert, P., Schenk, D., and Yednock, T. (2000) *Nat. Med.* **6,** 916–919
26. Bard, F., Barbour, R., Cannon, C., Carretto, R., Fox, M., Games, D.,

Guido, T., Hoenow, K., Hu, K., Johnson-Wood, K., Khan, K., Kholodenko, D., Lee, C., Lee, M., Motter, R., Nguyen, M., Reed, A., Schenk, D., Tang, P., Vasquez, N., Seubert, P., and Yednock, T. (2003) *Proc. Natl. Acad. Sci. U.S.A.* **100,** 2023–2028
27. DeMattos, R. B., Bales, K. R., Cummins, D. J., Dodart, J. C., Paul, S. M., and Holtzman, D. M. (2001) *Proc. Natl. Acad. Sci. U.S.A.* **98,** 8850–8855
28. Dodart, J. C., Bales, K. R., Gannon, K. S., Greene, S. J., DeMattos, R. B., Mathis, C., DeLong, C. A., Wu, S., Wu, X., Holtzman, D. M., and Paul, S. M. (2002) *Nat. Neurosci.* **5,** 452–457
29. Mohajeri, M. H., Saini, K., Schultz, J. G., Wollmer, M. A., Hock, C., and Nitsch, R. M. (2002) *J. Biol. Chem.* **277,** 33012–33017
30. Jawhar, S., Trawicka, A., Jenneckens, C., Bayer, T. A., and Wirths, O. (2010) *Neurobiol. Aging,* DOI:10.1016/j.neurobiolaging.2010.05.027
31. Kayed, R., Head, E., Thompson, J. L., McIntire, T. M., Milton, S. C., Cotman, C. W., and Glabe, C. G. (2003) *Science* **300,** 486–489
32. Gong, Y., Chang, L., Viola, K. L., Lacor, P. N., Lambert, M. P., Finch, C. E., Krafft, G. A., and Klein, W. L. (2003) *Proc. Natl. Acad. Sci. U.S.A.* **100,** 10417–10422
33. Cleary, J. P., Walsh, D. M., Hofmeister, J. J., Shankar, G. M., Kuskowski, M. A., Selkoe, D. J., and Ashe, K. H. (2005) *Nat. Neurosci.* **8,** 79–84
34. Shankar, G. M., Bloodgood, B. L., Townsend, M., Walsh, D. M., Selkoe, D. J., and Sabatini, B. L. (2007) *J. Neurosci.* **27,** 2866–2875
35. Klyubin, I., Betts, V., Welzel, A. T., Blennow, K., Zetterberg, H., Wallin, A., Lemere, C. A., Cullen, W. K., Peng, Y., Wisniewski, T., Selkoe, D. J., Anwyl, R., Walsh, D. M., and Rowan, M. J. (2008) *J. Neurosci.* **28,** 4231–4237
36. Marcello, A., Wirths, O., Schneider-Axmann, T., Degerman-Gunnarsson, M., Lannfelt, L., and Bayer, T. A. (2009) *Neurobiol. Aging,* DOI:10.1016/j.neurobiolaging.2009.08.011
37. Wirths, O., Breyhan, H., Schäfer, S., Roth, C., and Bayer, T. A. (2008) *Neurobiol. Aging* **29,** 891–901
38. Klein, W. L., Krafft, G. A., and Finch, C. E. (2001) *Trends in Neurosciences* **24,** 219–224
39. Selkoe, D. J. (2002) *Science* **298,** 789–791
40. Lambert, M. P., Barlow, A. K., Chromy, B. A., Edwards, C., Freed, R., Liosatos, M., Morgan, T. E., Rozovsky, I., Trommer, B., Viola, K. L., Wals, P., Zhang, C., Finch, C. E., Krafft, G. A., and Klein, W. L. (1998) *Proc. Natl. Acad. Sci. U.S.A.* **95,** 6448–6453
41. Walsh, D. M., Klyubin, I., Fadeeva, J. V., Cullen, W. K., Anwyl, R., Wolfe, M. S., Rowan, M. J., and Selkoe, D. J. (2002) *Nature* **416,** 535–539
42. Lesné, S., Koh, M. T., Kotilinek, L., Kayed, R., Glabe, C. G., Yang, A., Gallagher, M., and Ashe, K. H. (2006) *Nature* **440,** 352–357
43. Ono, K., Condron, M. M., and Teplow, D. B. (2009) *Proc. Natl. Acad. Sci. U.S.A.* **106,** 14745–14750
44. Shankar, G. M., Li, S., Mehta, T. H., Garcia-Munoz, A., Shepardson, N. E., Smith, I., Brett, F. M., Farrell, M. A., Rowan, M. J., Lemere, C. A., Regan, C. M., Walsh, D. M., Sabatini, B. L., and Selkoe, D. J. (2008) *Nat. Med.* **14,** 837–842
45. Lacor, P. N., Buniel, M. C., Furlow, P. W., Sanz Clemente, A. S., Velasco, P. T., Wood, M., Viola, K. L., and Klein, W. L. (2007) *J. Neurosci.* **27,** 796–807
46. Tomiyama, T., Matsuyama, S., Iso, H., Umeda, T., Takuma, H., Ohnishi, K., Ishibashi, K., Teraoka, R., Sakama, N., Yamashita, T., Nishitsuji, K., Ito, K., Shimada, H., Lambert, M. P., Klein, W. L., and Mori, H. (2010) *J. Neurosci.* **30,** 4845–4856
47. Lord, A., Englund, H., Söderberg, L., Tucker, S., Clausen, F., Hillered, L., Gordon, M., Morgan, D., Lannfelt, L., Pettersson, F. E., and Nilsson, L. N. (2009) *FEBS J.* **276,** 995–1006
48. Lord, A., Kalimo, H., Eckman, C., Zhang, X. Q., Lannfelt, L., and Nilsson, L. N. (2006) *Neurobiol. Aging* **27,** 67–77
49. Buttini, M., Masliah, E., Barbour, R., Grajeda, H., Motter, R., Johnson-Wood, K., Khan, K., Seubert, P., Freedman, S., Schenk, D., and Games, D. (2005) *J. Neurosci.* **25,** 9096–9101
50. Brody, D. L., and Holtzman, D. M. (2008) *Annu. Rev. Neurosci.* **31,** 175–193

Supplement Wirths et al.

Dot blot competition assay

PVDF membrane (Millipore) was activated in methanol for 3 seconds, washed with ddH2O and equilibrated in transfer buffer (25 mM Tris, 192 mM glycine, 20% methanol). AβpE3-38 (500 ng in H2O) was spotted on the wet PVDF membrane and left to dry for 10 minutes. After blocking of the membrane by 5% non-fat dry milk TBST solution the competitor antibodies 9D5 (IgG2b subclass) and 8C4 (IgG1 subclass) were diluted in 5% non-fat dry milk TBST solution (10 μg/ml) and incubated with the membrane over night at 4°C while gently shaking. Then the corresponding detector antibody (8C4 after pre-incubation with 9D5 and vice versa) was added (at 10 μg/ml) to each competitor antibody solution and incubated by gently shaking for two hours. After washing the membrane three times in 1xTBST for 15 minutes, IgG2b and IgG1 subclass-specific secondary antibodies conjugated to Cy3 (Jackson Immunoresearch) were diluted 1:200 in 5% non-fat dry milk TBST and used to cover the membrane probed with the 9D5 and 8C4 respectively with gentle shaking for one hour. Then the membrane was washed three times by 1xTBST for 15 minutes. Fluorescent dots were scanned using a Fuji CCD camera LAS-4000 mini and a fluorescence filter.

Immunostaining competition

Immunostaining on paraffin embedded sections was performed on 4 μm sagital paraffin sections, as described above. In order to study competition between 8C4 and 9D5, the specific binding sites of 8C4 (IgG1 subclass; 10 μg/ml) were blocked by application of the competitor antibody 9D5 (IgG2b subclass) (0.04 μg/ml) together with the non-specific treatment with skim milk and fetal calf serum in PBS, prior to the addition of the primary antibodies. Primary antibody 8C4 (10 μg/ml) was incubated overnight in a humid chamber at room temperature, followed by incubation with a IgG1 subclass specific secondary antibodies conjugated to Cy3 (Jackson Immunoresearch) diluted 1:200 in 5% non-fat dry milk TBST.

Supplementary Figure 1: 9D5 and 8C4 monoclonal antibodies were competing for the same epitope. (**A**) Parallel sections stained with 9D5 and 8C4 revealed indistinguishable pattern in two cases of sporadic AD showing either prominent blood vessel staining (sporadic case #1) or intraneuronal immunoreactivity (sporadic case #2). (**B**) 9D5 pre-incubation completely blocked 8C4 blood vessel staining in an AD case. (**C**) Dot blot competition assay. Significant lower 9D5 signal was detected after competition with 8C4 ($P<0.05$). The same was observed for the 8C4 signal after competition with 9D5 ($P<0.01$) by t-testing.

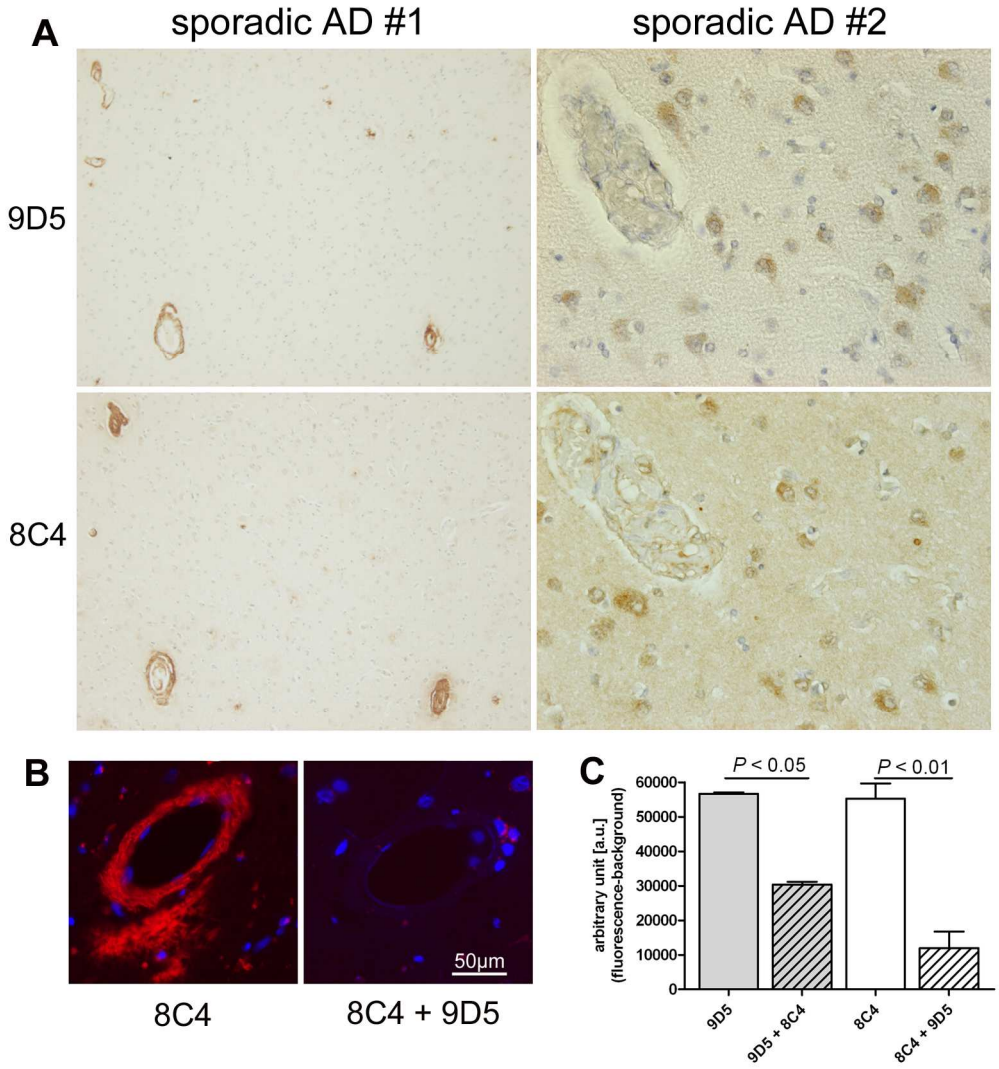

Supplementary Figure 2: 9D5 specifically recognizes AβpE3-42 by direct ELISA. 50 ng of each peptide was used. 9D5 did not recognize Aβ 1-7, Aβ1-16, Aβ1-38, Aβ1-40, Aβ1-42 or the N-terminal truncated peptide AβpE3-7.

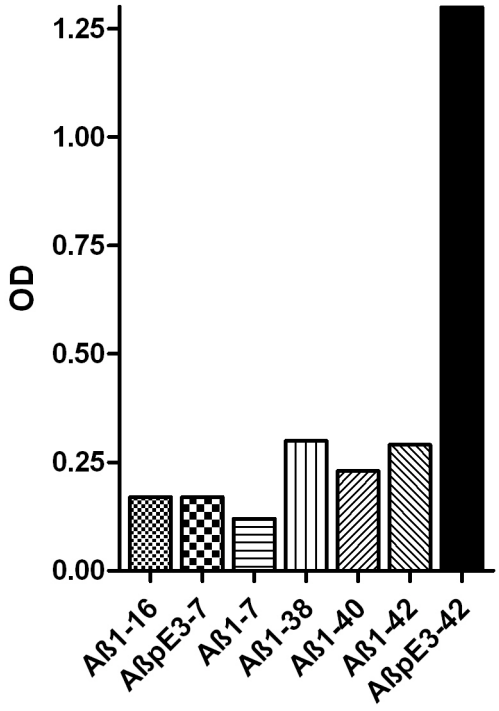

Supplementary Figure 3: 9D5 and 2-48 (against N-terminal AβpE3-x) monoclonal antibodies recognize a differential staining pattern. Adjacent sections of FAD case harboring the PS1 (Δexon9) mutation were stained with 2-48 (**A, A'**) and 9D5 (**B, B'**). While 2-48 recognized abundant plaques and vessel staining, 9D5 did not label plaques. The CAA staining did only partially overlap and was much less abundant compared to 2-48. Scale bars: A, B: 200µm; A`, B`: 50 µm.

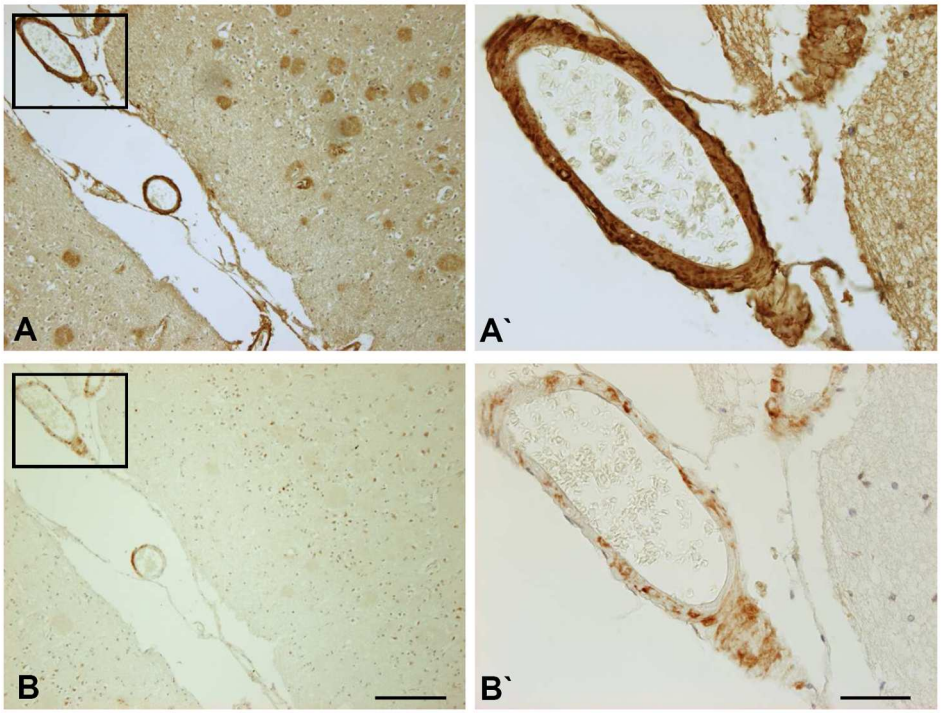

Supplementary Figure 4: 9D5 immunoreactivity in APP/PS1KI and APP single transgenic mice. In 2-month-old APP/PS1KI did not show any 9D5 immunoreactivity in the subiculum (**A**), whereas in 10-month-old APP/PS1KI mice abundant 9D5-staining could be detected (**B**). In cortical regions, abundant 9D5 staining could be detected already at the age of 6 month (**C**). In addition, strong intraneuronal 9D5 staining could be detected in spinal cord motor neurons at 12 months of age (**D**). 10-month-old APP single transgenic mice showed abundant 4G8 staining (**E**) and only minor 9D5-immunoreactivity (**F**). Age-matched APP/PS1KI bigenic mice harbouring mutant PS1 on a homozygous knock-in background showed strong 4G8 staining (**G**), as well as abundant 9D5 immunoreactivity (**H**). Scale bars: A,B: 200 μm; E-H: 100 μm; C,D: 50 μm

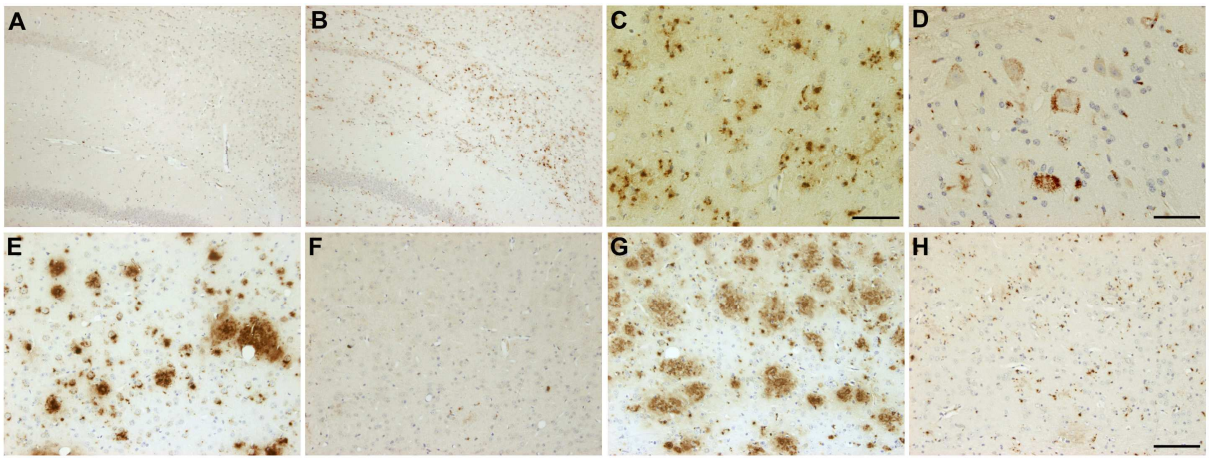

Supplementary Figure 5: Reduction of intracellular signal in the subiculum after passive immunisation of 5XFAD mice with 9D5. (**A**) Reduction of intracellular 9D5 immunoreactivity after passive immunisation with 9D5. (**B**) PBS treated 5XFAD mouse with intracellular 9D5 staining. 9D5-positive cells are indicated by arrows. Scale bar: 50 µm.

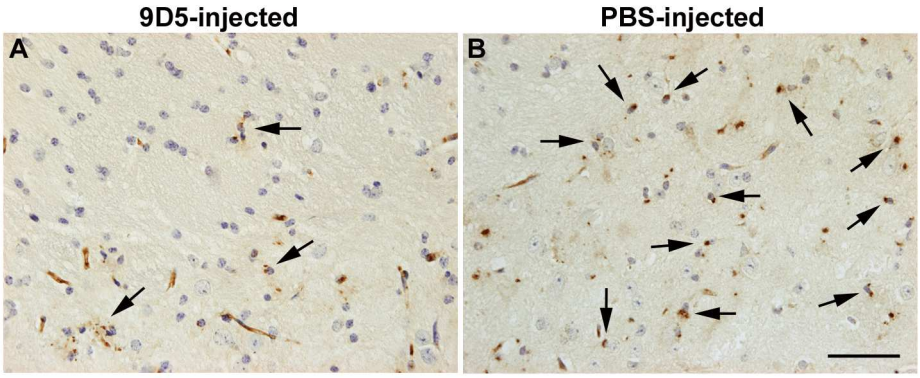

Supplementary Figure 6: Hypothesis of oligomeric AβpE3 pathology in Alzheimer disease brain. (**A**) In non-demented controls Aβ is secreted by neurons with no intraneuronal accumulation. Clearance of Aβ occurs by crossing blood brain barrier via the blood stream and/or brain derived Aβ degrading enzymes. (**B**) In AD oligomeric AβpE3 might be increased in brain parenchyma and blood vessels due to reduced blood brain barrier clearance. In addition, reduced secretion, impaired clearance mechanisms and/or transport problems might lead to intraneuronal aggregation of oligomeric AβpE3. AD cases harboring intraneuronal oligomeric AβpE3 might represent a certain state of the disease.

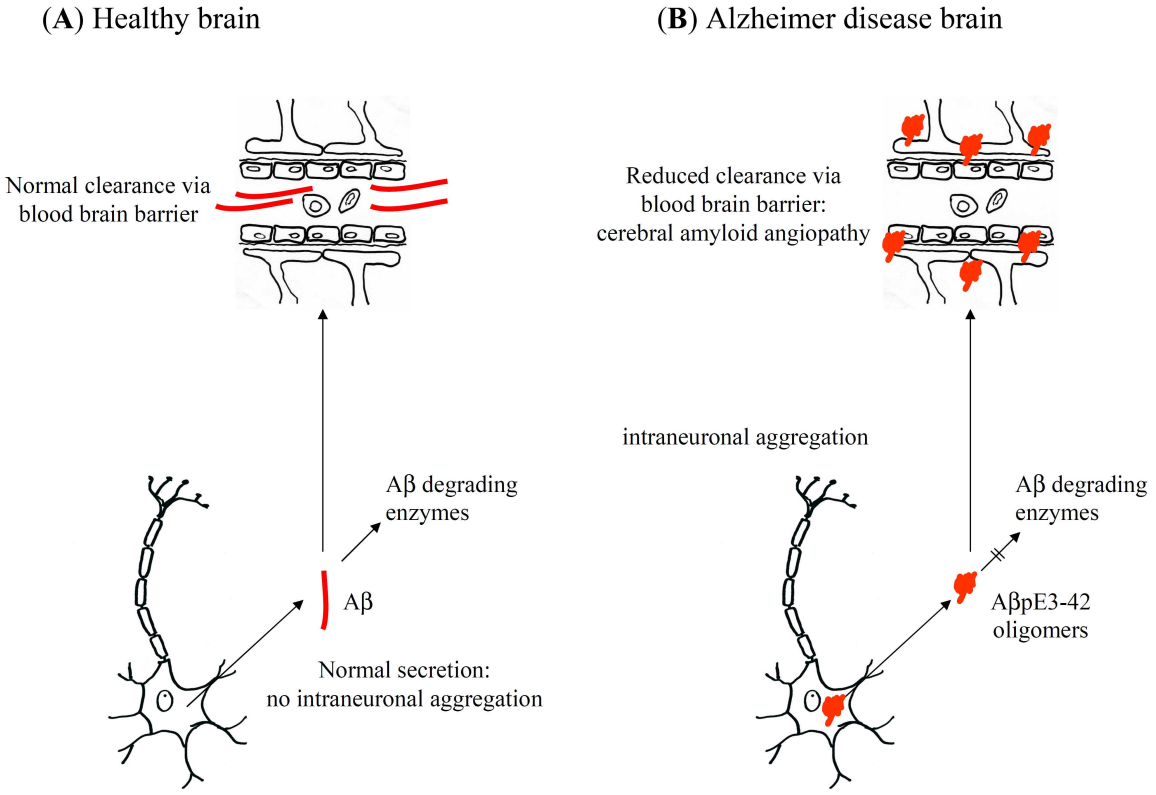

Supplementary Figure 7: Assessment of 9D5-positive neuropathological staining in sporadic (AD) and familial (FAD) Alzheimer disease patients with APP (arc, artic; swe, Swedish) and PS1 mutations ((P264L, L418F, Δexon9) and non-demented controls. ++, most if not all neurons, vessels or plaques were positive (**A**); +, weak to moderate staining of neurons (**B**), vessels (**C**) or plaques (**D**); (+) occasionally staining of neurons, vessels or plaques (**E**); -, no staining was detected (**F**).

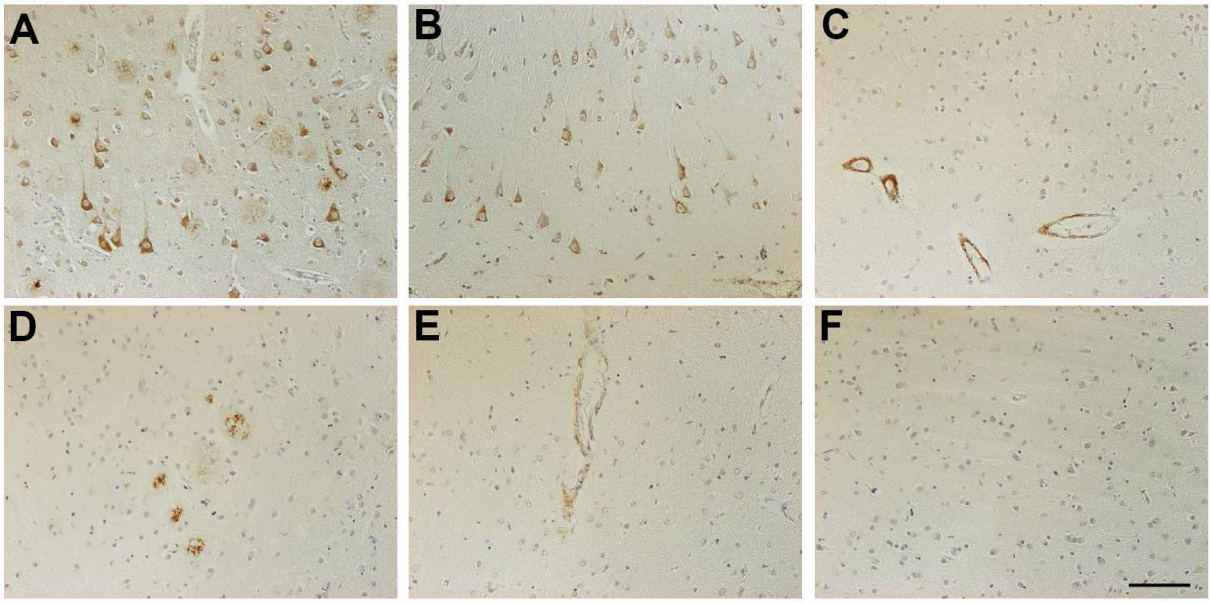

Supplementary Table 1. **Demographic data of sporadic (AD) and familial (FAD) Alzheimer disease patients with APP (arc, artic; swe, Swedish) and PS1 mutations ((P264L, L418F, Δexon9) and non-demented controls.** Oligomeric AβpE staining in sporadic and familial AD cases was observed in pyramidal neurons and blood vessels (CAA) of the hippocampus and frontal cortex. Minor plaque staining was only seen in some AD cases. Abbreviations: iAβ, intraneuronal Aβ; CAA, cerebral amyloid angiopathy; m, male; f, female; na, not analyzed; ++, most if not all neurons, vessels or plaques were positive; +, weak to moderate staining of neurons, vessels or plaques; (+) occasionally staining of neurons, vessels or plaques; -, no staining was detected (3 sections per case were analysed in a blinded fashion by the assessor).

			Oligomeric AβpE3				
	sex	age	iAβ	CAA	Plaques	Braak stage	ApoE
control	m	73	-	-	-	0	33
control	f	82	-	-	-	I	33
control	m	78	-	(+)	-	I	43
control	m	84	-	-	-	I	33
control	m	91	-	-	-	I	33
control	m	70	-	-	-	0	43
control	f	78	-	-	-	I	33
control	m	70	-	-	-	0	32
control	f	90	-	(+)	-	I	22
control	f	88	-	-	-	I	33
AD	f	79	+	+	+	IV	43
AD	m	93	-	+	-	IV	33
AD	f	86	-	+	-	IV	43
AD	f	86	-	-	-	IV	33
AD	m	86	-	(+)	+	IV	33
AD	m	92	-	-	-	IV	33
AD	f	92	-	(+)	-	IV	33
AD	f	88	-	-	-	IV	33
AD	f	85	+	-	-	IV	22
AD	f	88	-	(+)	-	IV	43
AD	m	81	-	+	+	IV	
AD	f	84	+	-	+	IV	32
AD	f	84	+	+	-	IV	43
AD	m	91	-	+	-	IV	42
AD	f	88	-	-	+	IV	33
AD	f	91	-	+	-	IV	43
AD	f	87	-	+	-	IV	43
AD	f	92	+	(+)	-	IV	42
AD	f	91	-	(+)	-	IV	43
AD	f	93	-	-	-	IV	33
FAD arc	m	64	(+)	+	+	na	na
FAD swe	f	61	(+)	++	+	na	na
FAD PS1 (P264L)	m	54	+	+	+	na	na
FAD PS1 (L418F)	m	38	++	-	++	na	na
FAD PS1 (Δexon9)	m	61	++	+	-	na	na
FAD PS1 (Δexon9)	m	64	++	+	-	na	33
FAD PS1 (Δexon9)	m	69	++	+	-	na	33